

Dissolution of residual tetrachloroethylene in fractional wettability porous media: Incorporation of interfacial area estimates

Scott A. Bradford

George E. Brown, Jr., Salinity Laboratory, U.S. Department of Agriculture, Riverside, California

Linda M. Abriola

Department of Civil and Environmental Engineering, University of Michigan, Ann Arbor, Michigan

Abstract. Available data from a recent study of entrapped tetrachloroethylene (PCE) dissolution [Bradford *et al.*, 1999] reveal that soil wettability and grain size distribution characteristics can dramatically influence dissolution behavior. This paper explores the modeling of the long-term dissolution of residual nonaqueous phase liquids (NAPLs) entrapped in fractional wettability porous media. Here dissolution is modeled with a linear driving force expression, and the lumped mass transfer coefficient is represented using independent estimates of the film mass transfer coefficient and the NAPL-water interfacial area. In fractional wettability porous media the NAPL saturation is assumed to occur as both NAPL films and ganglia, and NAPL-water interfacial area is thus modeled as the sum of contributions from films and ganglia. The interfacial area model is calibrated by fitting several parameters to the available experimental data. Trends in fitted parameters suggest that (1) residual NAPL ganglia are less accessible to a flowing aqueous phase in finer textured soils; (2) the dissolution rate depends on the interfacial area in a nonlinear manner; and (3) NAPL ganglia entrapment depends on system wettability and grain size distribution. Mass transfer coefficient correlations are established from these fitted parameters. The calibrated model predicts that for a given NAPL saturation, an increasing PCE-wet sand fraction results in longer periods of high effluent concentrations, followed by increased rates of concentration reduction and more persistent subsequent low-concentration tailing. The dependence of dissolution behavior on mean grain size is also captured by this model. Simulations demonstrate a significant improvement in dissolution predictions using the proposed model in comparison with those obtained using a previously developed mass transfer correlation based upon a power law function of saturation.

1. Introduction

Nonaqueous phase liquids (NAPLs) are commonly found at hazardous waste sites in many regions of the United States as a result of underground storage tank and piping leaks, surface spills, and improper disposal practices [Dragun *et al.*, 1984]. As a NAPL migrates through the subsurface, a residual portion is retained by the soil due to capillary forces. This entrapped NAPL serves as a persistent source of groundwater and/or air contamination because of its low solubility and often low volatility. Experimental and numerical studies have been undertaken to investigate the dissolution behavior of residual NAPLs [e.g., Pfannkuch, 1984; Hunt *et al.*, 1988; Geller and Hunt, 1993; Parker *et al.*, 1991; Miller *et al.*, 1990; Powers *et al.*, 1992; Guarnaccia *et al.*, 1992; Imhoff *et al.*, 1994, 1997; Powers *et al.*, 1991, 1992, 1994a, 1994b; Rixey, 1996]. Most of these studies have been conducted using water-wet glass beads or silica sands. Under water-wetting conditions, water occupies the smaller pores and pore spaces immediately adjacent to the soil grains in larger pores, and residual NAPL is entrapped in

the center of the larger pores as discontinuous ganglia or spherical singlets [Chatzis *et al.*, 1983]. Results from these studies indicate that dissolution behavior depends on system hydrodynamics, NAPL saturation and composition, and soil grain size distribution characteristics. Considerable discrepancies exist, however, among these experimental studies pertaining to the inferred degree of influence of soil grain size distribution parameters and NAPL saturation on dissolution behavior [cf. Miller *et al.*, 1998; Bradford *et al.*, 2000].

Researchers have suggested that rate-limited dissolution can occur under many circumstances [Hunt *et al.*, 1988; Borden and Kao, 1992; Powers *et al.*, 1992], i.e., for large multipore NAPL blobs, high aqueous phase velocities, low NAPL saturations, small mass fractions of soluble NAPL species, and residual NAPL found in “inaccessible” pores. The rate-limited mass transfer of the NAPL into the bulk aqueous phase has often been considered to be controlled by diffusion of the organic solute through an aqueous phase boundary layer at the NAPL-water interface [cf. de Zabala and Radke, 1986; Powers *et al.*, 1991]. In this case, a linear driving force model, a quasi steady state approximation of Fick’s first law, has been successfully used to describe dissolution behavior. According to this approach, the dissolution rate is the product of a lumped mass

Copyright 2001 by the American Geophysical Union.

Paper number 2000WR900374.
0043-1397/01/2000WR900374\$09.00

transfer coefficient (which is equal to the product of the film mass transfer coefficient and the NAPL-water interfacial area) and the concentration gradient across an aqueous phase boundary layer.

Correlation expressions for lumped mass transfer coefficients have been developed by a number of researchers based upon experimentally determined lumped mass transfer coefficients [e.g., *Pfannkuch*, 1984; *Parker et al.*, 1991; *Miller et al.*, 1990; *Powers et al.*, 1992; *Guarnaccia et al.*, 1992; *Imhoff et al.*, 1994, 1997]. These correlations typically incorporate system-specific values of the aqueous velocity, mean grain size, grain size distribution uniformity index, and residual NAPL saturation. A power function of the NAPL saturation is used as a surrogate parameter for temporal changes in NAPL-water interfacial area during dissolution [*Powers et al.*, 1994a; *Imhoff et al.*, 1994]. An alternative approach to the description of dissolution mass transfer utilizes independent estimates for the film mass transfer coefficient and the NAPL-water interfacial area [*Geller and Hunt*, 1993; *Powers et al.*, 1994b]. Often these estimates of the NAPL-water interfacial area have been obtained by assuming that the residual NAPL is entrapped as several sizes of spherical singlets with known radii [*Powers et al.*, 1994b; *Abriola et al.*, 1993]. A severe limitation of this approach is that knowledge of the ganglia size distribution is not readily available. Technologies such as photoluminescent volumetric imaging [*Montemagno and Gray*, 1995], interfacial tracers [*Saripalli et al.*, 1997; *Kim et al.*, 1997, 1999], and thermodynamic approaches [*Leverett*, 1941; *Morrow*, 1970; *Bradford and Leij*, 1997] may facilitate the measurement and/or estimation of interfacial areas. At present, however, little research has explored the use of interfacial area estimates in flow and transport studies. Both approaches to estimation of lumped mass transfer coefficients have been successfully applied to dissolution data for a limited range of NAPLs and porous media.

The above experimental and numerical modeling studies have been limited in their scope and application to water-wet systems. In many natural systems, however, the pore-scale distribution of residual NAPL may be much more complex due to spatial and temporal variations in wetting characteristics. The solid phase wettability is strongly dependent on the physical and chemical properties of the solid and fluid phases. For example, the wettability of natural soils depends on the solid phase mineralogy [*Anderson*, 1986], surface roughness [*Morrow*, 1975] and charge [*Hirasaki*, 1991], pH [*Zheng and Powers*, 1998], ionic composition [*Brown and Neustadter*, 1980] and strength [*Murphy et al.*, 1992], presence of organic acids [*Thomas et al.*, 1993] and bases [*Dubey and Doe*, 1993], and redox condition [*Wang and Guidry*, 1994]. In some instances, soils contain both water- and NAPL-wet solid surfaces. This condition is referred to as fractional wettability. The configuration of residual NAPL in fractional wettability systems can potentially include both multipore NAPL ganglia and singlets, as well as NAPL films. In the petroleum literature, fractional wettability has been recognized as a ubiquitous condition [*Brown and Fatt*, 1956; *Donaldson et al.*, 1969; *Salathiel*, 1973]. Heterogeneous distributions of water repellent soils are also a commonly reported phenomenon in the unsaturated zone [*DeBano*, 1969, 1981; *Letey et al.*, 1975; *Ma'shum et al.*, 1988; *Dekker and Ritsema*, 1994].

Recently, *Bradford et al.* [1999] presented entrapment and dissolution data for tetrachloroethylene (PCE) in soils representative of a range in grain size and fractional wettability characteristics. Experimental dissolution data indicate that for

a given NAPL saturation, an increase in the PCE-wet sand fraction results in longer periods of high effluent concentrations, followed by increased rates of concentration reduction and more persistent subsequent low-concentration tailing. For a given grain size distribution and NAPL saturation, an increase in the NAPL-wet fraction also resulted in a decrease in the dissolution time. This observation was attributed to enhanced mass transfer due to increases in interfacial area with increasing NAPL coverage of the solid surfaces [*Gvirtzman and Roberts*, 1991; *Bradford and Leij*, 1997]. The influence of fractional wettability on the dissolution behavior was also found to depend on the soil grain size distribution characteristics, especially for soils consisting of low PCE-wet mass fractions. PCE ganglia-film interactions provided a possible explanation for these observations [*Bradford et al.*, 1999].

To date, little research has addressed the modeling of NAPL dissolution behavior in fractional wettability porous media. *Bradford et al.* [2000] used a numerical simulator to analyze experimental fractional wettability dissolution data [*Bradford et al.*, 1999]. Owing to the inability of previously published mass transfer correlations to describe these data, these authors fitted a two-parameter power function model for the lumped mass transfer coefficient to the experimental data sets. Correlations were then developed for mass transfer model parameters as a function of wettability and grain size distribution characteristics. This power function model, in conjunction with the parameter correlations, yielded reasonable representations of long-term dissolution behavior in the more PCE-wetting media. Poorer model predictions for the more water-wet materials were attributed to an increased sensitivity of effluent concentration behavior to temporal changes in PCE saturation in these systems.

The primary objective of this work is to improve the description and prediction of the long-term dissolution behavior for NAPLs entrapped in fractional wettability porous media. Dissolution is modeled herein with a linear driving force model which utilizes estimates of the film mass transfer coefficient and the NAPL-water interfacial area. Interfacial area estimates follow from the procedure presented by *Bradford and Leij* [1997], while the film mass transfer coefficient is obtained from the correlation established by *Powers et al.* [1994b]. Model results are compared with experimental fractional wettability dissolution data [*Bradford et al.*, 1999], as well as with predictions based upon the lumped mass transfer correlation established by *Bradford et al.* [2000].

2. Conceptual Model of NAPL Dissolution

In fractional wettability porous media, the residual NAPL saturation (S_o) may be assumed to be the sum of contributions from NAPL entrapped as ganglia in water-wet pores (S_{og}) and as immobile films coating NAPL-wet solid surfaces (S_{of}). *Bradford et al.* [1998] postulated that S_{og} and S_{of} can be linearly related to the NAPL-wet sand mass fraction (F_o) as $(1 - F_o)S_o$ and F_oS_o , respectively. Recent analysis of measured residual NAPL saturation values and dissolution behavior in fractional wettability media, however, suggests that the magnitude of S_{og} and S_{of} vary in a more complex and nonlinear manner with F_o and soil grain size distribution [*Bradford et al.*, 1999]. In soils containing both NAPL ganglia and films, the values S_{og} and S_{of} will be more generally represented here as ωS_o and $(1 - \omega)S_o$, respectively, where ω is a fitted partitioning factor.

The following linear driving force expression is employed herein to describe the mass exchanged per unit time per unit volume between the NAPL and aqueous phases (E_{ow}):

$$E_{ow} = \frac{-\partial(\varepsilon S_o \rho_o)}{\partial t} = k_{ow}(\alpha A_{ow}^g + \beta A_{ow}^f)(C_s - C). \quad (1)$$

Here k_{ow} ($L T^{-1}$) is known as the film mass transfer coefficient; A_{ow}^g (L^{-1}) is the NAPL-water interfacial area per unit volume of porous media attributed to entrapped ganglia; A_{ow}^f (L^{-1}) is the NAPL-water interfacial area per unit volume of porous media attributed to residual NAPL films; C_s ($M L^{-3}$) is the equilibrium solubility concentration which approximates the concentration at the NAPL-water interface; C ($M L^{-3}$) is the bulk aqueous phase NAPL concentration; ε is the porosity; ρ_o ($M L^{-3}$) is the density of the NAPL; and α and β are fitting parameters. This form is an extension of that presented by Powers *et al.* [1994b], where α was introduced to account for the discrepancies between the actual residual NAPL shape and the idealized geometry and the fact that only a fraction of the interfacial area is exposed to mobile water. Note that most previous dissolution studies have modeled the lumped mass transfer coefficient ($K_{ow} = k_{ow}(\alpha A_{ow}^g + \beta A_{ow}^f)$) (T^{-1}) [e.g., Powers *et al.*, 1994a; Imhoff *et al.*, 1994, 1997]. In this work, independent estimates for the film mass transfer coefficient and interfacial areas will be sought.

According to Fick's first law, k_{ow} will be inversely related to the thickness of the NAPL-aqueous boundary layer and directly proportional to the diffusivity of the NAPL in the bulk aqueous phase. Consistent with experimental observations, however, the value of k_{ow} is typically modeled as a nonlinear function of diffusivity, velocity, and viscosity [Powers *et al.*, 1991]. In this work the value of k_{ow} will be estimated using a modified form of the dimensionless correlation developed by Powers *et al.* [1994b] from dissolution measurements of solid naphthalene spheres embedded in sandy porous media:

$$\begin{aligned} Sh = \frac{k_{ow} d_{50}}{D_L} &= 1.15 \left(\frac{\rho_w v_w d_{50}}{\mu_w} \right)^{0.654} \left(\frac{\mu_w}{D_L \rho_w} \right)^{0.486} \\ &= 1.15 Re^{0.654} Sc^{0.486}. \end{aligned} \quad (2)$$

Here the mean grain size d_{50} (L) is used as a surrogate characteristic length; μ_w ($M L^{-2} T^{-1}$) is the aqueous phase viscosity; ρ_w ($M L^{-3}$) is the density of the aqueous phase; v_w ($L T^{-1}$) is the aqueous phase pore water velocity; Sh is the Sherwood number; Re is the Reynolds number; and Sc is the Schmidt number. The above correlation was modified from that presented by Powers *et al.* [1994b] to account for the dependence of k_{ow} on $Sc = \mu_w/(\rho_w D_L)$ [Imhoff *et al.*, 1997]. Note that (2) assumes that the film mass transfer coefficient is independent of NAPL configuration. The influence of residual NAPL configuration on the lumped mass transfer coefficient is accounted for below by explicitly modeling temporal changes in the NAPL-water interfacial area.

An accurate representation of the evolving interfacial area is also essential for the prediction of the long-term dissolution behavior of residual NAPLs. The interfacial area attributed to the entrapped ganglia (A_{ow}^g) is determined herein by assuming that the NAPL is distributed among a number of ganglia classes (N). Each ganglia class (denoted with superscript j) consists of spherical singlets associated with a different saturation dependent radius (R^j) and NAPL saturation (S_{og}^{j*}) [Powers *et al.*, 1991; Powers *et al.*, 1994b]. The initial NAPL

ganglia saturation for a particular class (S_{og}^{j*}) was determined herein as $S_{og}^{j*} = S_{og}/N$. The interfacial area per unit volume for each pore class was determined as the product of the surface area of the sphere and the number of spheres per unit volume. Addition of the surface areas of the pore classes yields

$$A_{ow}^g = 3 \sum_{j=1}^N \frac{\varepsilon S_{og}^j}{R^j}. \quad (3)$$

The initial values of R^j (equation (3)) are estimated herein from NAPL-water capillary pressure (P_{ow})–water saturation (S_w) data using Laplace's equation for capillarity and assuming that the ganglia are entrapped in the largest portions of the pore space (i.e., in the saturation range $1 - S_{og} < S_w < 1$) [Bradford and Leij, 1997]. For this purpose, the saturation dependence of R^j is expressed below in terms of a corresponding initial water saturation of ganglia class j (S_w^{j*}) as

$$R^j(S_w^{j*}) = \frac{2\sigma_{ow} \cos(\phi_{sow})}{P_{ow}(S_w^{j*})} \quad 1 - S_{og} < S_w^{j*} < 1. \quad (4)$$

Here ϕ_{sow} is the solid-NAPL-water contact angle and σ_{ow} is the NAPL-water interfacial tension. Since ganglia are assumed to be entrapped in the largest portions of the pore space, S_w^{j*} is equal to $1 - S_{og} + (2j - 1)S_{og}^{j*}/2$ and $j = 1 \dots N$ [Bradford and Leij, 1997]. It is logical to assume that the initial ganglia sizes will be controlled by the size of the pore bodies (water imbibition) instead of the pore throats (water drainage). Hence main imbibition capillary pressure data were employed in (4). The main imbibition P_{ow} values in the saturation range $1 - S_{og} < S_w < 1$ were approximated herein as half the corresponding primary drainage P_{ow} values in this range [e.g., Kool and Parker, 1987]. In addition, since the pore radius distribution is independent of system wettability, P_{ow} - S_w data for similar (pore size distribution) water-wet soils having $\phi_{sow} \approx 0^\circ$ are used herein to predict A_{ow}^g for the fractional wettability soils.

Powers *et al.* [1992] measured the ganglia size distribution for styrene entrapped in several water-wet media. In these experiments the entrapped styrene ganglia were polymerized in situ, removed from the soil, and then sieved into various ganglia size classes. By assuming a spherical ganglia geometry, these authors estimated values for A_{ow}^g in a manner analogous to (3). For example, Ottawa 20-30 sand had a calculated A_{ow}^g equal to $3.52 \text{ cm}^2 \text{ cm}^{-3}$. Powers *et al.* [1992] also presents measured capillary pressure data for this sand. The use of (3) (assuming N equals 4) and (4) in conjunction with the reported capillary pressure parameters yields an estimate of the interfacial area at residual saturation equal to $3.15 \text{ cm}^2 \text{ cm}^{-3}$. The favorable agreement between these two estimates suggests that (3) provides a reasonable approximation of A_{ow}^g when using (4) to estimate R^j .

The value of A_{ow}^f at $1 - S_o$ can also be estimated from P_{ow} - S_w data. Thermodynamic considerations suggest that the area under a capillary pressure curve is related to the NAPL-water interfacial area [Leverett, 1941; Morrow, 1970; Bradford and Leij, 1997]. In this work an estimate of A_{ow}^f for a particular fractional wettability medium was obtained from primary drainage P_{ow} - S_w data for a water-wet medium with the same pore size distribution as

$$A_{ow}^f = -\frac{\varepsilon F_o}{\sigma_{ow}} \int_1^{S_{wmin}} P_{ow}(S) dS. \quad (5)$$

Here the limit of integration $S_{w\min}$ is the historic minimum water saturation and S is a dummy saturation variable of integration. In (5), film interfacial area is proportional to the interfacial area of drainage pore space and the fraction of organic-wet solids, F_o . This procedure is analogous to using the measured solid surface area and F_o to determine the NAPL-wet solid surface area, but it also accounts for the solid surface area exposed to NAPL.

Kim *et al.* [1997] and Saripalli *et al.* [1997] utilized interfacial tracers to estimate interfacial areas in several multiphase systems. These authors reported good agreement between their measured interfacial areas values and those predicted using techniques based upon the area under the capillary pressure curves. Although the fluid pairs and wettability conditions in these studies differ from those considered herein, their observations lend support to the use of estimation procedures similar to (5).

Equations (3), (4), and (5) provide initial estimates of the interfacial areas for a given residual NAPL saturation. Temporal changes in interfacial area as a result of dissolution must also be considered. It is assumed herein that as dissolution proceeds, changes in NAPL saturation (ΔS_o) during a given time interval are equal to the sum of changes in the NAPL ganglia (ΔS_{og}) and film (ΔS_{of}) saturations. When there are no interactions between NAPL ganglia and films, equation (1) indicates that the values of ΔS_{og} and ΔS_{of} will be related to the magnitudes of αA_{ow}^g and βA_{ow}^f as

$$\Delta S_o = \frac{\alpha A_{ow}^g}{\alpha A_{ow}^g + \beta A_{ow}^f} \Delta S_o + \frac{\beta A_{ow}^f}{\alpha A_{ow}^g + \beta A_{ow}^f} \Delta S_o$$

$$= \Delta S_{og} + \Delta S_{of}. \quad (6)$$

Note that the above values of ΔS_{og} and A_{ow}^g are actually divided into N subclasses according to (3); for simplicity only the sum of these contributions is shown in (6).

As dissolution progresses, the value of A_{ow}^f for a particular location is assumed to remain constant until S_{of} is zero, at which time A_{ow}^f is set equal to zero. This hypothesis is supported by experimental observations of transient volatilization [Abriola and Bradford, 1998] and dissolution [Bradford *et al.*, 1999] behavior when the NAPL is distributed as films. In contrast, the value of A_{ow}^g is modeled as an explicit function of saturation. In this case, the ganglia radii slowly decrease in size as S_{og} decreases. The saturation dependency of a particular ganglia class radius at a given location and time can be determined as

$$R^i(S_w^j) = R^i(S_w^*) \left(\frac{S_{og}^j}{S_{og}^*} \right)^{1/3}. \quad (7)$$

Equation (7) follows from the fact that the number of ganglia in a given class at a particular location remains constant during dissolution. Hence, as dissolution proceeds the ganglia size distribution will change spatially and temporally as a result of corresponding changes in the organic ganglia saturation. Once $R^i(S_w^j)$ is determined from (7), the updated interfacial area may be calculated directly from (3). Equation (4) is only used to estimate the initial ganglia radii.

The above conceptual model of dissolution was implemented in an existing numerical simulator, MGANGLIA [Bradford *et al.*, 2000]. MGANGLIA models one-dimensional organic solute transport in the aqueous phase, i.e., advection, hydrodynamic dispersion, and rate-limited dissolution and

sorption. Solute transport and NAPL and solid phase mass balance equations are approximated using a centered-difference discretization of the spatial terms and a fully implicit backward-difference discretization of the temporal terms. The set of coupled algebraic equations is solved sequentially using the Thomas algorithm, after implementing initial and boundary conditions. Nonlinear coefficients, including saturations and lumped mass transfer coefficients, are evaluated at the previous time level. The numerical implementation in MGANGLIA was verified by comparison of simulator output and results from one-dimensional analytical solutions and another one-dimensional NAPL dissolution simulator (GANGLIA) [Powers *et al.*, 1994a].

To facilitate the calibration of the above conceptual model with experimental data, MGANGLIA was incorporated into an optimization program based on the Levenberg-Marquardt algorithm [Bradford *et al.*, 2000]. This algorithm combines a quadratic-extrapolation strategy with a steepest descent approach to minimize the sum of the squared error between observed and predicted concentrations (the objective function) [Levenberg, 1944; Marquardt, 1963].

3. Applications

This section explores the ability of the above dissolution model to describe experimental dissolution data for residual tetrachloroethylene entrapped in fractional wettability porous media. The experimental entrapment and dissolution procedures and data analysis are presented and discussed in detail by Bradford *et al.* [1999]. In these experiments, fractional wettability soils were created by combining various mass fractions of untreated and octadecyltrichlorosilane (OTS) treated Ottawa sands. These soils will be designated herein by their sieve sizes (F20-F30, F35-F50, F70-F110, and F35-F50-F70-F110) and their NAPL-wet mass fraction F_o , or OTS percentage. The soil grain size distributions were characterized by their median grain size (d_{50}) and the uniformity index ($U_i = d_{60}/d_{10}$, where $x\%$ of the mass is finer than d_x). Table 1 summarizes the wettability, grain size distribution parameters, porosity, residual organic saturation, and the aqueous phase Darcy velocity (q) for the experimental systems employed in this study. The fluids consisted of Milli-Q water and laboratory grade (99%) tetrachloroethylene (Aldrich Chemical Co., Milwaukee, Wisconsin). PCE has a density of 1.623 g cm^{-3} , a viscosity of 0.89 cP [Lide, 1994], an interfacial tension of 45.0 dyn cm^{-1} with water [Brown *et al.*, 1994], an equilibrium solubility (C_s) of approximately 203 mg L^{-1} at 20°C [Bradford *et al.*, 1999], and an aqueous phase diffusion coefficient of $6.56 \times 10^{-6} \text{ cm}^2 \text{ s}^{-1}$ [Hayduk and Laudie, 1974].

Estimates of the initial interfacial area for the various sand systems considered herein were obtained with equations (3), (4), and (5) using measured P_{ow} - S_w data. PCE-water P_{ow} - S_w curves were obtained using an automated setup [Bradford and Leij, 1995a] based upon the pressure cell approach; i.e., saturations change in response to imposed boundary conditions until equilibrium conditions are achieved. The soil columns and packing procedures were identical to those employed in the entrapment and dissolution experiments presented by Bradford *et al.* [1999]. Figure 1 presents all primary drainage PCE-water P_{ow} - S_w data and fitted *van Genuchten* [1980] P_{ow} - S_w model curves for the completely water wet sands. These curves were used to estimate A_{ow}^g and A_{ow}^f according to (3) (assuming N equals 4) and (5), respectively. Values of

Table 1. Properties of Experimental Systems

F_o	U_i	d_{50} , cm	q , cm min ⁻¹	ε	S_o	A_{ow}^* , cm ⁻¹
<i>F20-F30</i>						
0.00	1.21	0.071	0.516	0.327	0.128	4.808
0.10	1.21	0.071	0.466	0.318	0.055	7.086
0.25	1.21	0.071	0.481	0.324	0.057	18.036
0.50	1.21	0.071	0.503	0.337	0.059	37.494
0.75	1.21	0.071	0.512	0.342	0.026	57.076
<i>F35-F50</i>						
0.00	1.88	0.036	0.451	0.321	0.111	7.554
0.10	1.88	0.036	0.480	0.314	0.098	12.297
0.25	1.88	0.036	0.471	0.341	0.061	33.330
0.50	1.88	0.036	0.487	0.341	0.071	66.277
0.75	1.88	0.036	0.551	0.325	0.053	94.750
1.00	1.88	0.036	0.470	0.341	0.062	132.553
<i>F35-F50-F70-F110</i>						
0.00	3.06	0.024	0.480	0.302	0.114	7.694
0.10	3.06	0.024	0.497	0.301	0.132	15.701
0.25	3.06	0.024	0.500	0.294	0.074	38.235
0.50	3.06	0.024	0.520	0.298	0.050	77.510
0.75	3.06	0.024	0.499	0.313	0.096	122.118
1.00	3.06	0.024	0.509	0.306	0.118	159.182
<i>F70-F110</i>						
0.00	2.25	0.015	0.549	0.316	0.143	25.236
0.10	2.25	0.015	0.493	0.326	0.150	31.556
0.25	2.25	0.015	0.481	0.342	0.087	61.546
0.50	2.25	0.015	0.455	0.340	0.101	122.157
0.75	2.25	0.015	0.481	0.346	0.093	186.469
1.00	2.25	0.015	0.479	0.348	0.245	250.062

S_{wmin} that were utilized in (5) were determined from the measured capillary pressure curves shown in Figure 1 (S_{wmin} equals 0.02, 0.065, 0.16, and 0.30 for the F20-F30, F35-F50, F35-F50-F70-F110, and F70-F110 soils, respectively). Table 1 also provides initial estimates of the total interfacial area per unit volume of porous media ($A_{ow}^* = A_{ow}^g + A_{ow}^f$) for the various soils utilized in this study. These estimates follow directly from (3) and (5) given a value of ω . Fitted values of ω that were utilized for this purpose will be discussed in the next section. Note in Table 1 that the value of A_{ow}^* for a particular

soil increases with increasing organic-wet mass fraction. Also observe that for a particular level of fractional wettability, the value of A_{ow}^* increases with decreasing mean soil grain size.

3.1. Model Calibration

The conceptual model of NAPL dissolution presented above requires specification of the number of ganglia size classes, N (see equation (3)). A sensitivity analysis of dissolution behavior in the water-wet soils was used to establish a value for N . This analysis consisted of running simulations for a particular soil

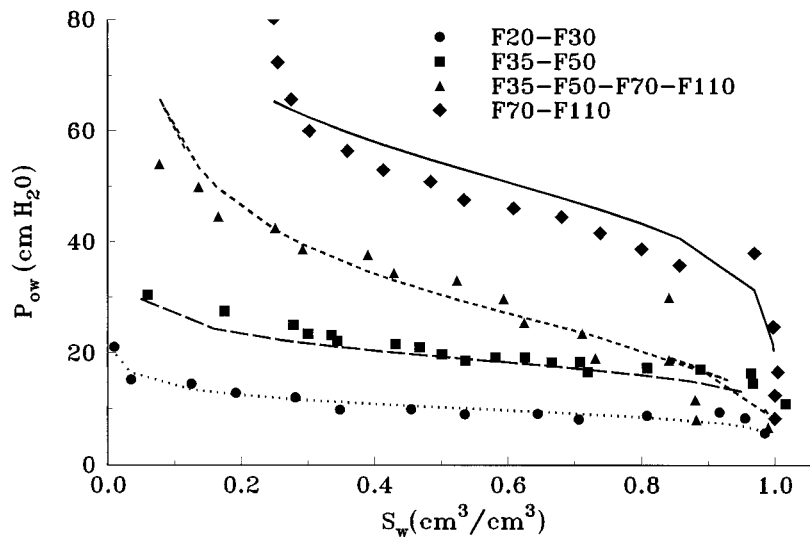


Figure 1. Primary drainage PCE-water P_{ow} - S_w data and van Genuchten [1980] P_{ow} - S_w model curve fits for the completely water wet sands that were used to estimate A_{ow}^g and A_{ow}^f according to equations (3) and (5), respectively.

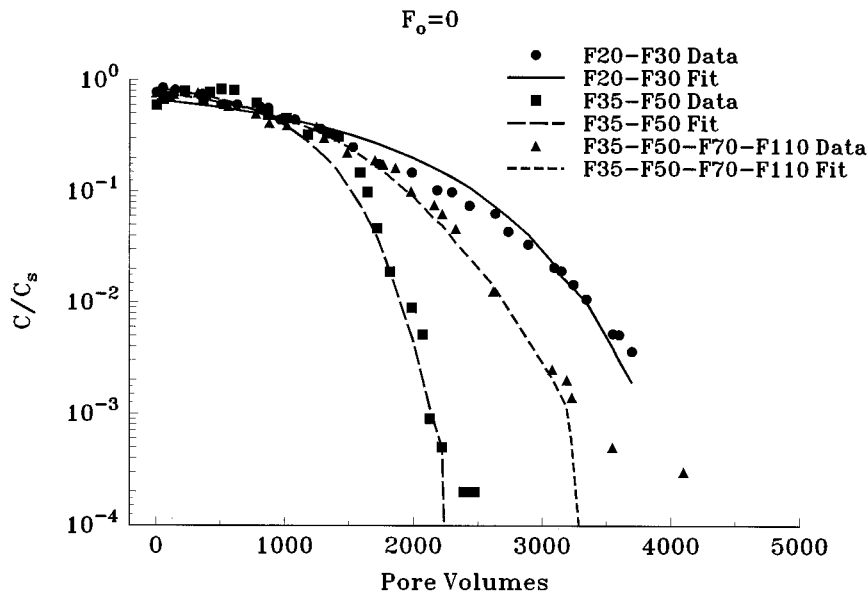


Figure 2. Observed and best fit (α) effluent concentration curves for PCE entrapped in the indicated water-wet porous media.

system using various values of N (ranging from 1 to 7). The simulated effluent curves were observed to asymptotically approach a limiting effluent concentration curve as N increased. In more uniform soils, lower N values were required to reach this limiting curve. On the basis of this sensitivity analysis, a value of N equal to 4 was selected for the porous media considered herein.

The conceptual model also includes three fitting parameters (ω , α , and β). Measured concentration data were used to develop correlations for these fitting parameters. In this effort, only effluent concentrations ranging between the equilibrium solubility and 3 orders of magnitude below this value were considered. Bradford *et al.* [1999] demonstrated that the observed low-concentration tailing, $C/C_s < 10^{-3}$, in fractional wettability dissolution experiments was likely due to rate-limited desorption of PCE from the OTS-treated sands. Bradford *et al.* [2000] found that this desorption behavior could be adequately modeled using a linear driving force expression in conjunction with measured equilibrium sorption data. Thus no attempt was made to fit this tailing in the work described herein, and sorption is neglected.

In water-wet porous media, only the parameter α needs to be determined, since $S_o = S_{og}$ ($\omega = 1$) and $A_{ow}^f = 0$. The parameter α theoretically accounts for the discrepancies between the actual ganglia shape and the assumed spherical geometry and the fact that only a fraction of the interfacial area is exposed to mobile water [Powers *et al.*, 1994b]. Figure 2 presents observed and fitted effluent concentrations curves for the selected water-wet sand systems. Here (2) was used to estimate k_{ow} . Hence the shape of the effluent curve is primarily controlled by spatial and temporal changes in the ganglia interfacial area. The interfacial area slowly decreases with decreasing ganglia saturation. Table 2 summarizes best fit values of α as well as the coefficient of linear regression (r^2), the mean square error (MSE), and the 95% confidence interval on the fitted parameter determined according to the Student's *t*-test [e.g., Samuels, 1989]. The single parameter fit models the

data well over the 3 order of magnitude concentration range considered (Figure 2).

A correlation between the fitted values of α and grain size distribution characteristics (mean grain size and distribution uniformity coefficient) was sought to facilitate the prediction of the measured dissolution data. A variety of functional forms for the correlation were tested and evaluated. Because only four fitted α values were available, a single parameter correlation was sought. The previously discussed nonlinear least squares fitting routine was used for this purpose. The value of α was found to depend on the normalized mean grain size ($\delta = d_{50}/0.05$) as

$$\alpha = -\frac{0.1052}{\delta} + 0.3957 \quad r^2 = 0.996. \quad (8)$$

Note that this correlation is strictly valid over the range of experimental mean grain sizes ($0.071 \geq d_{50} \geq 0.015$ cm) used in correlation development; for $\delta < 0.266$ the value of α is physically unrealistic (negative). Equation (8) indicates that the value of α decreases with decreasing d_{50} . This suggests that in finer-texture porous media, less mobile water contacts the NAPL ganglia or that dissolution fingering is more pronounced [Imhoff and Miller, 1996; Imhoff *et al.*, 1996].

In porous media where $S_o = S_{of}$ ($\omega = 0$) and $A_{ow}^g = 0$, only β needs to be fit. It is reasonable to assume that $S_o = S_{of}$ in porous media having $F_o \geq 0.50$, since any ganglia formed in such media could be drained by the presence of NAPL films on adjacent sand grains. Figure 3 presents examples of observed and fitted effluent concentration curves for several soils having $F_o \geq 0.5$. Here effluent concentration values are near equilibrium levels until the NAPL films are completely dissolved. Table 2 summarizes best fit values of β and statistical parameters for the goodness of the fit. Note the good agreement between observed and fitted curves (Figure 3), as well as the high coefficient of linear regression and low mean square error (Table 2).

Table 2. Best Fit Model Parameters and Statistical Values for the Goodness of Fit

F_o	Parameter	Fit	r^2	MSE	-95%	+95%
<i>F20-F30</i>						
0.00	α	0.3261	0.9293	0.0063	0.3195	0.3327
0.10	ω	0.0107	0.8196	0.0179	0.0159	0.0055
0.25	ω	0.0131	0.9838	0.0026	0.0213	0.0049
0.50	β	0.0832	0.9811	0.0030	0.0753	0.0911
0.75	β	0.0515	0.9954	0.0007	0.0471	0.0560
<i>F35-F50</i>						
0.00	α	0.2506	0.9048	0.0096	0.2485	0.2528
0.10	ω	0.3077	0.9111	0.0107	0.3228	0.2926
0.25	ω	0.0754	0.9827	0.0024	0.0796	0.0712
0.50	β	0.0436	0.9837	0.0026	0.0415	0.0458
0.75	β	0.0304	0.9973	0.0004	0.0284	0.0324
1.00	β	0.0240	0.9853	0.0023	0.0234	0.0246
<i>F35-F50-F70-F110</i>						
0.00	α	0.1658	0.9832	0.0012	0.1562	0.1754
0.10	ω	0.1152	0.8632	0.0106	0.2622	0.0000
0.25	ω	0.0300	0.9490	0.0050	0.0338	0.0262
0.50	β	0.0164	0.9679	0.0027	0.0140	0.0189
0.75	β	0.0146	0.9754	0.0037	0.0123	0.0169
1.00	β	0.0117	0.9785	0.0033	0.0104	0.0130
<i>F70-F110</i>						
0.00	α	0.0551	0.9153	0.0078	0.0535	0.0567
0.10	ω	0.3348	0.9393	0.0066	0.3381	0.3314
0.25	ω	0.0112	0.9896	0.0016	0.0156	0.0067
0.50	β	0.0156	0.9972	0.0005	0.0152	0.0161
0.75	β	0.0106	0.9929	0.0012	0.0098	0.0114
1.00	β	0.0091	0.9224	0.0113	0.0088	0.0095

Figure 4 plots the variability of β with A_{ow}^f . Note that the value of β tends to decrease asymptotically with increasing A_{ow}^f . A correlation between the fitted values of β and A_{ow}^f and grain size distribution characteristics was sought to facilitate the prediction of the measured dissolution data. The previously discussed nonlinear least squares fitting routine was used. The value of β was found to depend on A_{ow}^f and grain size distribution uniformity coefficient (U_i) as

$$\beta = 2.104 \times A_{ow}^{f-0.844} U_i^{-0.915} \quad r^2 = 0.962. \quad (9)$$

Recall that A_{ow}^f is related to P_{ow} - S_w data according to (5). Hence (9) can also be rewritten in terms of fitted P_{ow} - S_w model parameters using an analytic solution of (5) [e.g., Brooks and Corey, 1964].

The inverse dependence of β on U_i in (9) suggests that some of the residual NAPL films are less accessible to a flowing

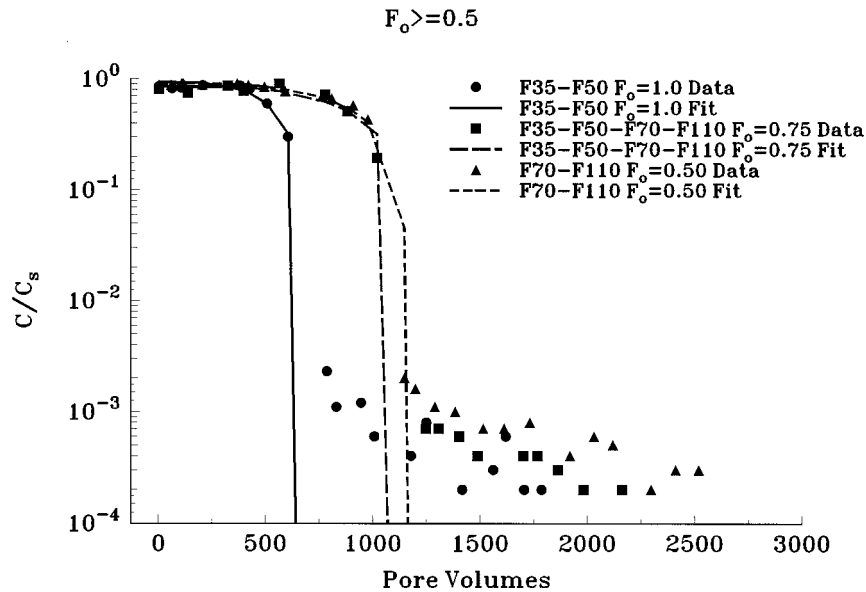


Figure 3. Observed and best fit (β) effluent concentration curves for PCE entrapped in the indicated $F_o \geq 0.50$ porous media.

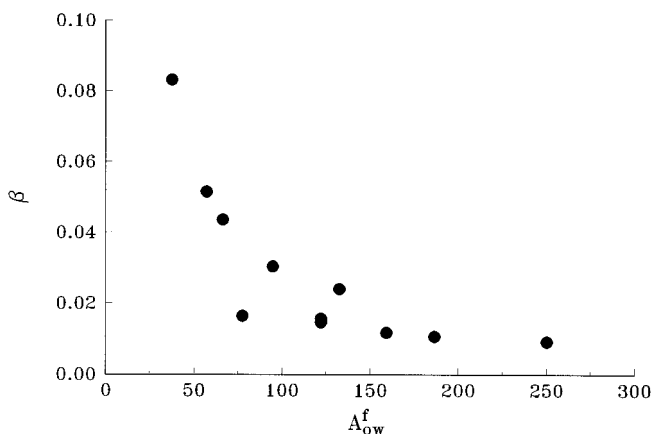


Figure 4. A plot of fitted values of β as a function of the initial nonaqueous phase liquid film interfacial area.

aqueous phase in more graded soils. The value of β is also inversely proportional to A_{ow}^f . This result is somewhat surprising since it seems inconsistent with (1), which states that the dissolution rate is directly proportional to A_{ow}^f when $A_{ow}^g = 0$. Equation (9) suggests, then, that $K_{ow} = \beta A_{ow}^f$ is proportional to A_{ow}^f raised to the power 0.156 under organic wetting conditions ($A_{ow}^g = 0$). One possible explanation is that system hydrodynamics and fluid properties limit the maximum value of K_{ow} , such that further increases in A_{ow}^f do not affect K_{ow} . For example, water flowing in larger pores may never reach the equilibrium solubility limit regardless of the system interfacial area, provided that the fluid residence time is low or fluid mixing is incomplete. Hence the product of β and A_{ow}^f may be viewed as accounting for the nonlinear influence of A_{ow}^f on the dissolution rate. In support of these hypothesis, *Wilkins et al.* [1995] observed that the volatilization rates for NAPL entrapped in the unsaturated zone (NAPL films on the air-residual water interface) were proportional to the mean grain size. Since the surface area is inversely related the mean grain

size, this finding also suggests a nonlinear correlation between volatilization rates and interfacial area.

In soils containing residual NAPL entrapped as both ganglia and films, estimates of $S_{og} = \omega S_o$ and $S_{of} = (1 - \omega)S_o$ must be obtained. In order to quantify S_{og} and S_{of} , values of ω were fit to dissolution data sets from soils having F_o equal to 0.10 or 0.25. To avoid nonuniqueness problems, the values of α and β were estimated from the correlations presented in (8) and (9), respectively. Figure 5 presents observed and fitted effluent concentration curves for several soils having $F_o = 0.1$ or 0.25. Table 2 summarizes best fit values of ω and statistical parameters for the goodness of the fit. In general, good agreement between observed and fitted curves (Figure 5 and Table 2) are achieved. This observation suggests that the proposed conceptual model of dissolution and entrapment can accurately capture the dissolution behavior of entrapped NAPL in fractional wettability porous media.

Figure 6 presents a plot of the variation of the fitted $\omega = S_{og}/S_o$ with F_o for the various soil types. Note that ω equals unity for $F_o = 0$ by definition and then rapidly goes to zero as F_o increases. One possible explanation for this behavior is that NAPL-wet solid surfaces hinder the formation of NAPL ganglia; i.e., ganglia that would otherwise form near water-wet solids are drained by the presence of NAPL films on adjacent sand grains. The rate of decrease also depends on the soil grain size distribution characteristics. When $F_o = 0.1$, the value of ω is much lower for the F20-F30 soil than for the other finer-textured soils. This distinct difference in ω when $F_o = 0.1$ suggests that ganglia entrapment was diminished further in the coarser F20-F30 sand as a result of decreasing capillary forces. *Morrow et al.* [1988] found that entrapment of residual ganglia decreased above a threshold capillary (ratio of viscous to capillary forces) or bond (ratio of gravitational to capillary forces) number. Unfortunately, their analysis was limited to water-wet systems, and no systematic studies have been conducted to explore the influence of capillary, viscous, and gravitational forces on ganglia entrapment for different porous medium wettabilities.

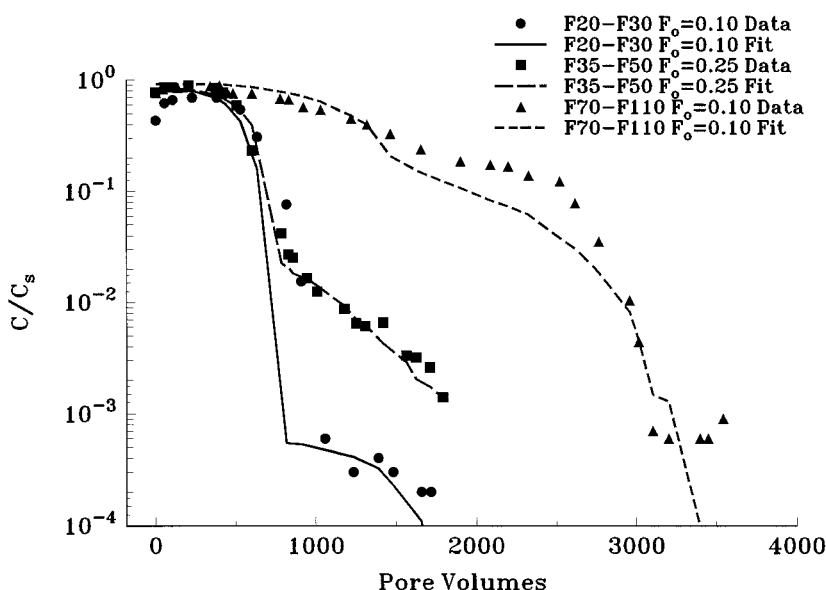


Figure 5. Observed and best fit (ω) effluent concentration curves for PCE entrapped in the indicated soils have F_o equal to 0.10 or 0.25.

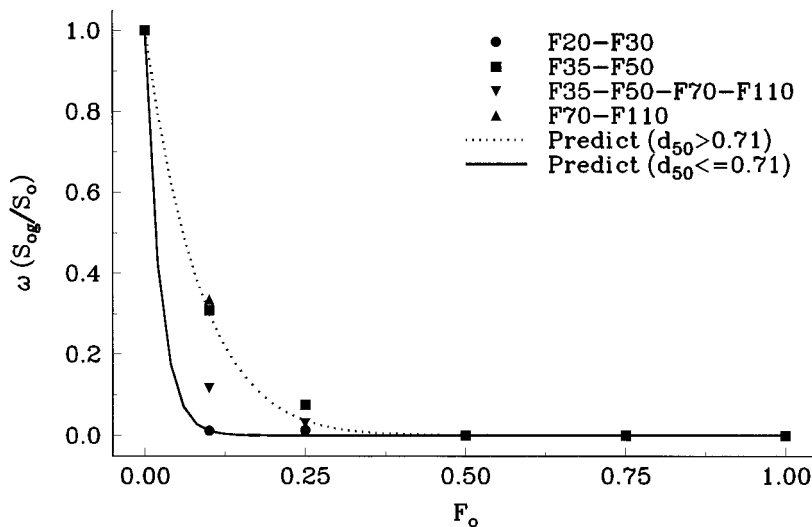


Figure 6. A plot of fitted and predicted values of $\omega = S_{og}/S_o$ as a function of F_o for the indicated soils.

On the basis of the fitted values of ω shown in Figure 6, the following empirical correlations were developed:

$$\begin{aligned} \omega &= (1 - F_o)^{11.44} & d_{50} < 0.071 \\ \omega &= (1 - F_o)^{42.79} & d_{50} \geq 0.071. \end{aligned} \quad (10)$$

Equations (10) assume that ganglia entrapment ($\omega = S_{og}/S_o$) depends on system wettability and a threshold mean grain size (capillary force). Below the threshold mean grain size ($d_{50} < 0.71$), ganglia entrapment is controlled primarily by the porous media wettability. Above this threshold mean grain size ($d_{50} \geq 0.71$), ganglia entrapment is further hindered as a result of decreasing capillary forces. Note that values of S_{of}/S_o can also be determined from (10) as $1 - \omega$. The above correlation predictions are also presented in Figure 6, demonstrating that the correlation provides a reasonable description of the data. The coefficient of linear regression was determined to be 0.960. A more precise description of ganglia entrapment would require a systematic investigation of ganglia entrapment over a range of capillary, viscous, and gravitational forces in soils of various wettabilities. Such an investigation is beyond the scope of this paper.

3.2. Predictions

In this section the ability of the calibrated entrapment and dissolution model to predict experimental data will be investigated. Unfortunately, independent dissolution data for NAPL entrapped in fractional wettability porous media are presently unavailable. Hence the “predictions” for the NAPL dissolution data presented below are not completely independent, since these same data were also used in the correlation development.

The fractional wettability dissolution data that were utilized herein to calibrate the proposed dissolution model were also recently used by Bradford *et al.* [2000] to develop the following correlation for the lumped mass transfer coefficient:

$$Sh^* = \frac{K_{ow}d_{50}^2}{D_L} = 0.254\delta^{0.475}U_i^{-1.187}Re^{0.654}Sc^{0.486}\left(\frac{\theta_o}{\theta_{io}}\right)^\gamma, \quad (11)$$

where $\gamma = 0.959(1 - F_o)^{6.265/U_i}$.

Here θ_o is the volumetric organic content; θ_{io} is the initial volumetric organic liquid content; and Sh^* is a slightly different form of the Sherwood number equal to $(K_{ow}d_{50}^2)/D_L$. Similar to previously established correlations for lumped mass transfer coefficients in water-wet soils [i.e., Powers *et al.*, 1994a; Imhoff *et al.*, 1994, 1997], (11) uses a simple volumetric NAPL content power function as a surrogate parameter for temporal changes in interfacial area. The initial dissolution rate is a function of grain size distribution parameters, as well as of Reynolds and Schmidt numbers.

Figures 7a, 7b, and 7c present the observed and predicted effluent concentration curves for PCE entrapped in the indicated soils. Here predictions are based upon the correlation expressions presented herein. For comparison, dissolution predictions using (11) to determine the lumped mass transfer coefficient are also shown in these figures. Note that the observed dissolution behavior and remediation times are fairly accurately described by the model developed in this work (see equations (1)–(10)). Consistent with the experimental data, the model predicts that for a given NAPL saturation, an increasing PCE-wet sand fraction results in longer periods of high effluent concentrations, followed by increased rates of concentration reduction. The model also captures the observed sensitivity of the dissolution data to grain size distribution characteristics. The predictions for the low NAPL-wet percentage soils shown in Figure 7c were, however, sometimes described less adequately than the other dissolution data sets. In comparison, dissolution predictions according to (11) provided only a good description for effluent curves in more PCE-wetting media. Bradford *et al.* [2000] attributed this observation to an increased sensitivity of effluent concentration behavior to temporal changes in PCE saturation in these systems. Note, however, that predictions using the model developed herein, equations (1)–(10), are always superior to those using (11). This is especially true for soils containing lower NAPL-wet mass fractions. The model proposed herein is, however, more difficult to implement and requires additional data input.

Figure 8 presents effluent concentration behavior for the $F_o = 0.1$ F20-F30 sand for various values of $\omega = S_{og}/S_o$.

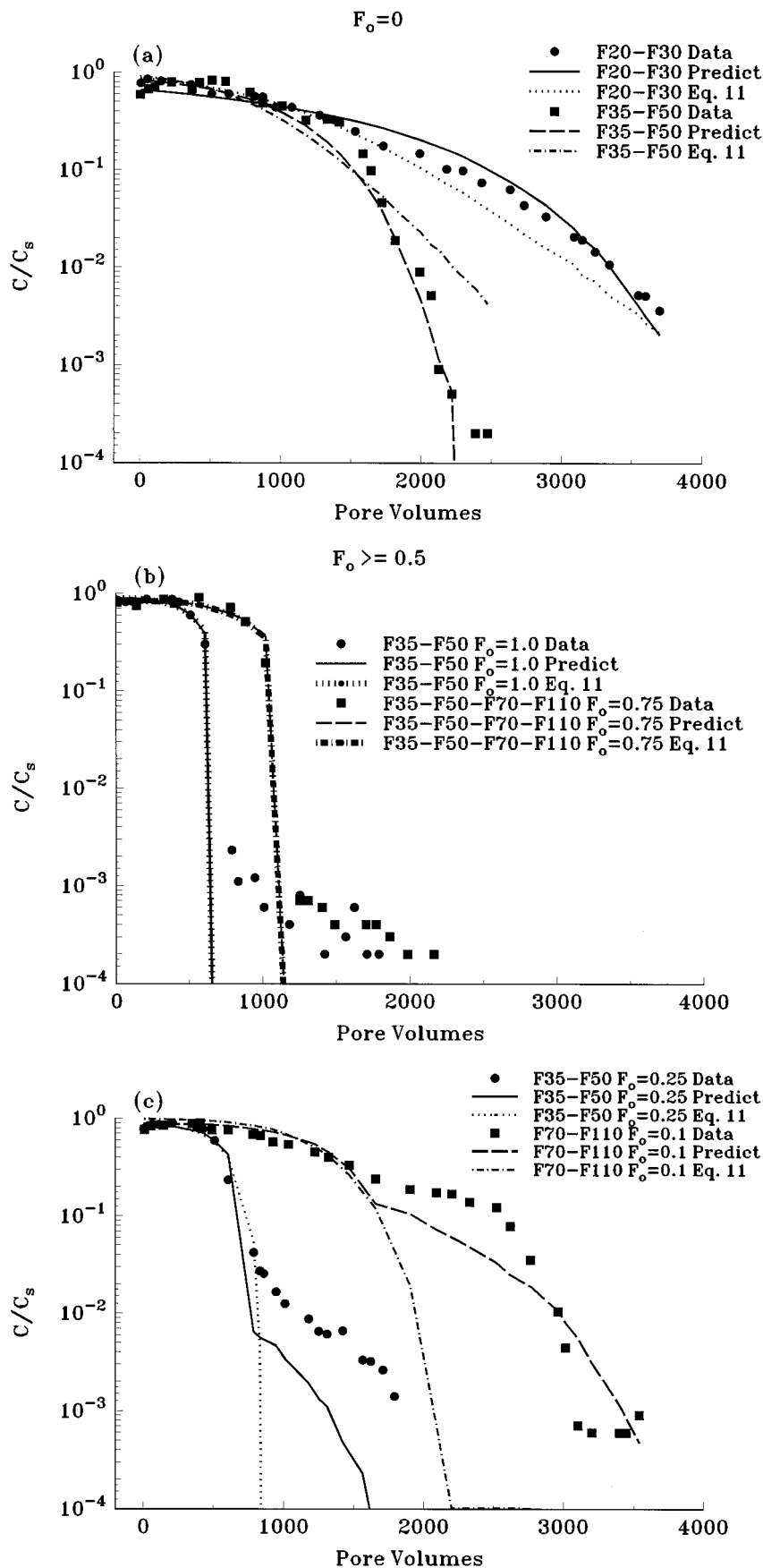


Figure 7. Observed and predicted effluent concentration curves for PCE entrapped in the indicated soils. Here predictions are shown for the model developed herein, equations (1)–(10), and those based upon the lumped mass transfer correlation established by Bradford *et al.* [2000] (see equation (11)).

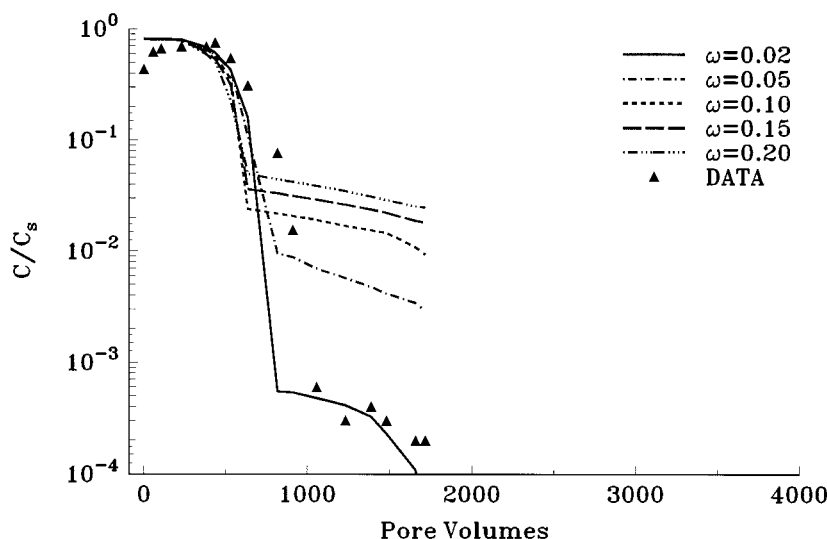


Figure 8. Predicted effluent concentration behavior for the F20-F30 $F_o = 0.1$ sand for various values of ω .

Note that the predicted dissolution behavior depends strongly on the value of ω . Increasing ω significantly increases the concentration tailing and hence the remediation time. In contrast, decreases in ω lead to longer periods of high initial effluent concentrations and hence shorter remediation times. This observation suggests that most of the differences in observed and predicted (see equations (1)–(10)) dissolution behavior for the lower NAPL-wet fractions soils (Figure 7c) are due to inaccuracies in the estimation of S_{og} (see equation (10)).

The use of (5) and (10) requires an estimate of F_o . In this work the value of F_o is known and equal to the OTS-treated sand mass fraction. No methods currently exist, however, to independently estimate the NAPL-wet fraction of natural soils. It may be possible, however, to correlate traditional wettability indices with known OTS fraction to provide a relatively simple means of estimating the “equivalent” OTS fraction of a particular soil. Some of these wettability indices are the United States Bureau of Mines (USBM) index (I_{usbm}) [Donaldson *et al.*, 1969; Sharma and Wunderlich, 1985], the Amott-Harvey index [Boneau and Clampitt, 1977], the water drop penetration time [Letey *et al.*, 1975], and the air-water imbibition rate [Powers and Tamblin, 1995]. For example, Bradford and Leij [1995b] established a correlation between I_{usbm} and F_o .

4. Summary and Conclusions

This paper presents a conceptual model to describe the entrapment and long-term dissolution behavior of residual NAPL in fractional wettability porous media. Rate-limited dissolution is modeled with a linear driving force expression. The residual NAPL, and hence the interfacial area, is assumed to be the sum of contributions from NAPL ganglia and films. Estimates of the film mass transfer coefficient and the NAPL-water interfacial area are utilized in the model to determine the lumped mass transfer coefficient. Interfacial area estimates are generally based upon the procedure presented by Bradford and Leij [1997], while the film mass transfer coefficient was obtained from a modified form of the correlation established by Powers *et al.* [1994b].

The model was calibrated by fitting several parameters to

the fractional wettability dissolution data of Bradford *et al.* [1999]. In water-wet porous media the fitting parameter α was used to account for discrepancies between the actual ganglia shape and the assumed spherical geometry and the fact that only a fraction of the interfacial area is exposed to mobile water. The fitted values of α were observed to decrease with decreasing mean grain size. This suggests that in finer-texture porous media, less mobile water contacts the NAPL ganglia. In media containing only NAPL films the fitting parameter β was found to be inversely related to the grain size distribution uniformity coefficient and the NAPL film interfacial area. This observation suggests that some of the residual NAPL films are less accessible to a flowing aqueous phase in more graded soils and suggests a nonlinear dependence of dissolution rate on interfacial area. In media containing both NAPL films and ganglia the partition factor, $\omega = S_{og}/S_o$, was fit to experimental dissolution data. The value of ω was found to be a function of both the mean grain size and the NAPL-wet sand mass fraction. Fitted values suggest that NAPL ganglia entrapment depends on system wettability and a threshold mean grain size (capillary force). Below a threshold mean grain size, ganglia entrapment is controlled primarily by the porous media wettability. Above this threshold mean grain size, ganglia entrapment is hindered or ganglia mobilization occurs.

Correlations for the fitting parameters were successfully established. This calibrated entrapment and dissolution model was then used to “predict” the fractional wettability dissolution data of Bradford *et al.* [1999]. Owing to limited experimental fractional wettability dissolution data, these predictions were not completely independent, since the same experimental data were also used in correlation development. Consistent with the experimental data, the model predicts that for a given NAPL saturation, an increase in the NAPL-wet fraction results in longer periods of high effluent concentrations, followed by increased rates of concentration reduction and finally low-concentration tailing. The model also predicts the observed sensitivity of the dissolution data to grain size distribution characteristics. The dependence of the dissolution behavior on the NAPL-wet sand fraction and the grain size distribution characteristics is embedded in the estimates of interfacial area,

the NAPL ganglia saturation, the film mass transfer coefficient, and the correlations developed from the fitting parameters that were utilized herein. Comparison of the dissolution data and model predictions revealed a reasonable agreement, suggesting that the conceptual model of NAPL ganglia and films accurately captures the dissolution behavior. In the case of the low NAPL-wet sand fraction systems, the agreement was sometimes unsatisfactory owing to the sensitivity of the predicted dissolution behavior to estimates of the NAPL ganglia saturation. Simulations demonstrate, however, that the model developed in this work provides a more accurate prediction of PCE dissolution in the considered soils than predictions based upon the lumped mass transfer correlation recently presented by Bradford *et al.* [2000]. This is especially true for soils containing lower NAPL-wet mass fractions. The proposed model is, however, more difficult to implement and requires additional data input.

Dissolution data and model predictions presented herein demonstrate that fractional wettability and grain size distribution characteristics can dramatically influence the long-term dissolution behavior of residual NAPLs. There is presently a need to quantify wettability parameters in natural soils and subsurface formations and to investigate dissolution behavior in heterogeneous natural environments. Future studies will investigate the influence of coupled physical and chemical heterogeneity on the entrapment and dissolution behavior of residual NAPLs. The extension of the dissolution model presented herein to such systems, as well as to media containing entrapped and pooled NAPL, warrants further examination.

Acknowledgments. Funding for this research was provided by the National Institute of Environmental Health Sciences under grant ES04911 and by the Department of Energy under grant DE-FG07-96ER14702. The research described in this article has not been subject to Agency review and therefore does not necessarily reflect the views of the Agency, and no official endorsement should be inferred. The authors thank Tom Phelan for his assistance in the modeling aspects of this work and Richard Vendlinski and Dave Doezeema in providing laboratory assistance.

References

- Abriola, L. M., and S. A. Bradford, Experimental investigations of the entrapment and persistence of organic liquid contaminants in the subsurface environment, *Environ. Health Perspect.*, **106**, 1083–1095, 1998.
- Abriola, L. M., T. J. Dekker, and K. D. Pennell, Surfactant-enhanced solubilization of residual dodecane in soil columns, 2, Mathematical modelling, *Environ. Sci. Technol.*, **27**, 2341–2351, 1993.
- Anderson, W. G., Wettability literature survey, part 1, Rock/oil/brine interactions and the effects of core handling on wettability, *J. Pet. Technol.*, **38**, 1125–1144, 1986.
- Boneau, D. F., and R. L. Clappitt, Determination of oil saturation after waterflooding in an oil-wet reservoir—The north bank unit, Tract 97 project, *J. Pet. Technol.*, **29**, 491–500, 1977.
- Borden, R. C., and C.-M. Kao, Evaluation of groundwater extraction for remediation of petroleum-contaminated aquifers, *Water Environ. Res.*, **64**, 28–36, 1992.
- Bradford, S. A., and F. J. Leij, Wettability effects on scaling two- and three-fluid capillary pressure-saturation relations, *Environ. Sci. Technol.*, **29**, 1446–1455, 1995a.
- Bradford, S. A., and F. J. Leij, Fractional wettability effects on two- and three-fluid capillary pressure-saturation relations, *J. Contam. Hydrol.*, **20**, 89–109, 1995b.
- Bradford, S. A., and F. J. Leij, Estimating interfacial areas for multi-fluid soil systems, *J. Contam. Hydrol.*, **27**, 83–105, 1997.
- Bradford, S. A., L. M. Abriola, and K. M. Rathfelder, Flow and entrapment of dense nonaqueous phase liquids in physically and chemically heterogeneous aquifer formations, *Adv. Water Resour.*, **22**, 117–132, 1998.
- Bradford, S. A., R. A. Vendlinski, and L. M. Abriola, The entrapment and long-term dissolution of tetrachloroethylene in fractional wettability porous media, *Water Resour. Res.*, **35**, 2955–2964, 1999.
- Bradford, S. A., T. J. Phelan, and L. M. Abriola, Dissolution of residual tetrachloroethylene in fractional wettability porous media: Correlation development and application, *J. Contam. Hydrol.*, **45**, 35–61, 2000.
- Brooks, R. H., and A. T. Corey, Hydraulic properties of porous media, *Hydrol. Pap.* 3, Colo. State Univ., Fort Collins, 1964.
- Brown, C. E., and E. L. Neustadter, The wettability of oil/water/silica systems with reference to oil recovery, *J. Can. Pet. Technol.*, **19**, 100–110, 1980.
- Brown, R. J. S., and I. Fatt, Measurements of fractional wettability of oilfield rocks by the nuclear magnetic relaxation method, *Trans. Am. Inst. Min. Metall. Pet. Eng.*, **207**, 262–264, 1956.
- Brown, C. L., G. A. Pope, L. M. Abriola, and K. Sepehrnoori, Simulation of surfactant-enhanced aquifer remediation, *Water Resour. Res.*, **30**, 2959–2977, 1994.
- Chatzis, I., N. R. Morrow, and H. T. Lim, Magnitude and detailed structure of residual oil saturation, *Soc. Pet. Eng. J.*, **23**, 311–326, 1983.
- DeBano, L. F., Water repellent soils: A worldwide concern in management of soil and vegetation, *Agric. Sci. Rev.*, **7**, 11–18, 1969.
- DeBano, L. F., Water repellent soils: A state of the art, *Gen. Tech. Rep. PSW-46*, 21 pp., Pac. Southwest For. and Range Exp. Stn., U.S. Dep. of Agric., Berkeley, Calif., 1981.
- Dekker, L. W., and C. J. Ritsema, How water moves in a water repellent sandy soil, 1, Potential and actual water repellency, *Water Resour. Res.*, **30**, 2507–2519, 1994.
- de Zabala, E. F., and C. J. Radke, A non-equilibrium description of alkaline water flooding, *SPE Reservoir Eng.*, **2**, 29–43, 1986.
- Donaldson, E. C., R. D. Thomas, and P. B. Lorenz, Wettability determination and its effect on recovery efficiency, *Soc. Pet. Eng. J.*, **9**, 13–20, 1969.
- Dragun, J., A. C. Kuffner, and R. W. Schreiner, Groundwater contamination, part I, Transport and transformations of organic chemicals, *Chem. Eng.*, **91**, 65–70, 1984.
- Dubey, S. T., and P. H. Doe, Base number and wetting properties of crude oils, *SPE Reservoir Eng.*, **9**, 195–200, 1993.
- Geller, J. T., and J. R. Hunt, Mass transfer from nonaqueous phase organic liquids in water-saturated porous media, *Water Resour. Res.*, **29**, 833–846, 1993.
- Guarnaccia, J. F., P. T. Imhoff, B. C. Missildine, M. Oostrom, M. A. Celia, J. H. Dane, P. R. Jaffe, and G. F. Pinder, Multiphase chemical transport in porous media, final report, *EPA/600/S-92/002*, U.S. Environ. Prot. Agency, Washington, D. C., 1992.
- Gvrtzman, H., and P. V. Roberts, Pore scale spatial analysis of two immiscible fluids in porous media, *Water Resour. Res.*, **27**, 1165–1176, 1991.
- Hayduk, W., and H. Laudie, Prediction of diffusion coefficients for nonelectrolytes in dilute aqueous solutions, *AIChE J.*, **20**, 611–615, 1974.
- Hirasaki, G. J., Wettability: Fundamentals and surface forces, *SPE Form. Eval.*, **6**, 217–226, 1991.
- Hunt, J. R., N. Sitar, and K. S. Udell, Nonaqueous phase liquid transport and cleanup, 1, Analysis of mechanisms, *Water Resour. Res.*, **24**, 1247–1258, 1988.
- Imhoff, P. T., and C. T. Miller, Dissolution fingering during the solubilization of nonaqueous phase liquids in saturated porous media, 1, Model predictions, *Water Resour. Res.*, **32**, 1919–1928, 1996.
- Imhoff, P. T., P. R. Jaffe, and G. F. Pinder, An experimental study of complete dissolution of a nonaqueous phase liquid in a saturated porous media, *Water Resour. Res.*, **30**, 307–320, 1994.
- Imhoff, P. T., G. P. Thyrum, and C. T. Miller, Dissolution fingering during the solubilization of nonaqueous phase liquids in saturated porous media, 2, Experimental observations, *Water Resour. Res.*, **32**, 1929–1942, 1996.
- Imhoff, P. T., A. Frizzell, and C. T. Miller, Evaluation of thermal effects on the dissolution of a nonaqueous phase liquid in porous media, *Environ. Sci. Technol.*, **31**, 1615–1622, 1997.
- Kim, H., P. S. Rao, and M. D. Annable, Determination of effective air-water interfacial area in partially saturated porous media using surfactant adsorption, *Water Resour. Res.*, **33**, 2705–2711, 1997.
- Kim, H., P. S. C. Rao, and M. D. Annable, Consistency of the inter-

- facial tracer technique: Experimental evaluation, *J. Contam. Hydrol.*, 40, 79–94, 1999.
- Kool, J. B., and J. C. Parker, Development and evaluation of closed-form expressions for hysteretic soil hydraulic properties, *Water Resour. Res.*, 23, 105–114, 1987.
- Leteý, J., J. F. Osborn, and N. Valoras, Soil water repellency and the use of nonionic surfactants, *Contrib. 154*, Calif. Water Resour. Cent., Davis, 1975.
- Levenberg, K., A method for the solution of certain non-linear problems in least squares, *Q. Appl. Math.*, 2, 164–168, 1944.
- Leverett, M. C., Capillary behavior in porous solids, *Trans. Am. Inst. Min. Metall. Pet. Eng.*, 142, 152–169, 1941.
- Lide, D. R., *CRC Handbook of Chemistry and Physics*, 5th ed., CRC Press, Boca Raton, Fla., 1994.
- Marquardt, D. W., An algorithm for least-squares estimation of non-linear parameters, *J. Soc. Ind. Appl. Math.*, 11, 431–441, 1963.
- Ma'shum, M., M. E. Tate, G. P. Jones, and J. M. Oades, Extraction and characterization of water-repellent materials from Australian soils, *J. Soil Sci.*, 39, 99–109, 1988.
- Miller, C. T., M. M. Poirier-McNeill, and A. S. Mayer, Dissolution of trapped nonaqueous phase liquids: Mass transfer characteristics, *Water Resour. Res.*, 26, 2783–2796, 1990.
- Miller, C. T., G. Christakos, P. T. Imhoff, J. F. McBride, J. A. Pedit, and J. A. Trangenstein, Multiphase flow and transport modeling in heterogeneous porous media: Challenges and approaches, *Adv. Water Resour.*, 21, 77–120, 1998.
- Montemagno, C. D., and W. G. Gray, Photoluminescent volumetric imaging: A technique for the exploration of multiphase flow and transport in porous media, *Geophys. Res. Lett.*, 22, 425–428, 1995.
- Morrow, N. R., Physics and thermodynamics of capillary action in porous media, in *Flow Through Porous Media*, edited by R. J. M. de Wiest, pp. 104–128, Academic, San Diego, Calif., 1970.
- Morrow, N. R., The effects of surface roughness on contact angle with special reference to petroleum recovery, *J. Can. Pet. Technol.*, 14, 42–53, 1975.
- Morrow, N. R., I. Chatzis, and J. J. Taber, Entrapment and mobilization of residual oil in bead packs, *SPE Reservoir Eng.*, 4, 927–934, 1988.
- Murphy, E. M., J. M. Zachara, S. C. Smith, and J. L. Phillips, The sorption of humic acids to mineral surfaces and their role in contaminant binding, *Sci. Total Environ.*, 117/118, 413–423, 1992.
- Parker, J. C., A. K. Katyal, J. J. Kaluarachchi, R. J. Lenhard, T. J. Johnson, K. Jayaraman, K. Jayaraman, K. Unlu, and J. L. Zhu, Modeling multiphase organic chemical transport in soils and ground water, final report, *EPA/600/2-91/042*, U.S. Environ. Prot. Agency, Washington, D. C., 1991.
- Pfannkuch, H. O., Ground-water contamination by crude oil at the Bemidji, Minnesota, research site: U.S. Geological Survey toxic water-ground-water contamination study, paper presented at the Toxic-Waste Technical Meeting, U.S. Geol. Surv., Tucson, Ariz., March 20–22, 1984.
- Powers, S. E., and M. E. Tamblin, Wettability of porous media after exposure to synthetic gasolines, *J. Contam. Hydrol.*, 19, 105–125, 1995.
- Powers, S. E., C. O. Loureiro, L. M. Abriola, and W. J. Weber Jr., Theoretical study of the significance of nonequilibrium dissolution of nonaqueous phase liquids in subsurface systems, *Water Resour. Res.*, 27, 463–477, 1991.
- Powers, S. E., L. M. Abriola, and W. J. Weber Jr., An experimental investigation of NAPL dissolution in saturated subsurface systems: Steady state mass transfer rates, *Water Resour. Res.*, 28, 2691–2705, 1992.
- Powers, S. E., L. M. Abriola, and W. J. Weber Jr., An experimental investigation of NAPL dissolution in saturated subsurface systems: Transient mass transfer rates, *Water Resour. Res.*, 30, 321–332, 1994a.
- Powers, S. E., L. M. Abriola, J. S. Dunkin, and W. J. Weber Jr., Phenomenological models for transient NAPL-water mass-transfer processes, *J. Contam. Hydrol.*, 16, 1–33, 1994b.
- Rixey, W. G., The long-term dissolution characteristics of a residually trapped BTX mixture in soil, *Hazard. Waste Hazard. Mater.*, 13, 197–211, 1996.
- Salathiel, R. A., Oil recovery by surface film drainage in mixed wettability rocks, *J. Pet. Technol.*, 25, 1216–1224, 1973.
- Samuels, M. L., *Statistics for the Life Sciences*, Macmillan, Old Tappan, N. J., 1989.
- Saripalli, K. P., H. Kim, P. S. C. Rao, and M. D. Annable, Use of interfacial tracers to measure immiscible fluid interfacial areas in porous media, *Environ. Sci. Technol.*, 31, 932–936, 1997.
- Sharma, M. M., and R. W. Wunderlich, The alteration of rock properties due to interactions with drilling fluid components, paper presented at the Society of Petroleum Engineers Annual Technical Conference and Exhibition, Las Vegas, Nev., Sept. 22–25, 1985.
- Thomas, M. M., J. A. Clouse, and J. M. Longo, Adsorption of organic compounds on carbonate minerals, 1, Model compounds and their influence on mineral wettability, *Chem. Geol.*, 109, 201–213, 1993.
- van Genuchten, M. T., A closed form equation for predicting the hydraulic conductivity of unsaturated soils, *Soil Sci. Soc. Am. J.*, 44, 892–898, 1980.
- Wang, H. L., and L. J. Guidry, Effect of oxidation-reduction condition on wettability alteration, *SPE Form. Eval.*, 9, 140–148, 1994.
- Wilkins, M. D., L. M. Abriola, and K. D. Pennell, An experimental investigation of rate-limited NAPL volatilization in unsaturated porous media: Steady state mass transfer, *Water Resour. Res.*, 31, 2159–2172, 1995.
- Zheng, J., and S. E. Powers, Organic bases in NAPLs and their impact on wettability, *J. Contam. Hydrol.*, 39, 161–181, 1999.

L. M. Abriola, Department of Civil and Environmental Engineering, University of Michigan, 181 EWRE, 1351 Beal Avenue, Ann Arbor, MI 48109-2125.

S. A. Bradford, George E. Brown, Jr., Salinity Laboratory, U.S. Department of Agriculture, ARS, 450 West Big Springs Road, Riverside, CA 92507-4617.

(Received March 16, 2000; revised September 5, 2000; accepted November 14, 2000.)

